

# UC Davis

## UC Davis Previously Published Works

### Title

Adamantyl-ureas with pyrazoles substituted by fluoroalkanes as soluble epoxide hydrolase inhibitors

### Permalink

<https://escholarship.org/uc/item/7cj8n6pw>

### Authors

Burmistrov, Vladimir V  
Morisseau, Christophe  
Shkineva, Tatyana K  
et al.

### Publication Date

2023-02-01

### DOI

10.1016/j.jfluchem.2023.110087

Peer reviewed



Published in final edited form as:

*J Fluor Chem.* 2023 February ; 266: . doi:10.1016/j.jfluchem.2023.110087.

## Adamantyl-ureas with pyrazoles substituted by fluoroalkanes as soluble epoxide hydrolase inhibitors

Vladimir V. Burmistrov<sup>a,b,\*</sup>, Christophe Morisseau<sup>a</sup>, Tatyana K. Shkineva<sup>c</sup>, Dmitry V. Danilov<sup>b</sup>, Boris Gladkikh<sup>b</sup>, Gennady M. Butov<sup>b</sup>, Robert R. Fayzullin<sup>d</sup>, Tatyana Ya. Dutova<sup>c</sup>, Bruce D. Hammock<sup>a</sup>, Igor L. Dalinger<sup>c</sup>

<sup>a</sup>Department of Entomology and Nematology, and Comprehensive Cancer Center, University of California, Davis, CA, 95616, USA

<sup>b</sup>Department of Chemistry, Technology and Equipment of Chemical Industry, Volzhsky Polytechnic Institute (branch) Volgograd State Technical University, 42a Engels Street, Volzhsky, 404121, Russia

<sup>c</sup>N.D. Zelinsky Institute of Organic Chemistry, Russian Academy of Sciences, 47 Lenin Avenue, Moscow 119991, Russia

<sup>d</sup>Arbuzov Institute of Organic and Physical Chemistry, FRC Kazan Scientific Center, Russian Academy of Sciences, 8 Arbuzov Street, Kazan, 420088, Russia

### Abstract

A series of soluble epoxide hydrolase (sEH) inhibitors containing halogenated pyrazoles was developed. Inhibition potency of the obtained compounds ranges from 0.8 to 27.5 nM. 1-Adamantyl-3-[(4,5-dichloro-1-methyl-1H-pyrazol-3-yl)methyl]urea (**3f**, IC<sub>50</sub> = 0.8 nM) and 1-[(Adamantan-1-yl)methyl]-3-[(4,5-dichloro-1-methyl-1H-pyrazol-3-yl)methyl]urea (**4f**, IC<sub>50</sub> = 1.2 nM) were found to be the most potent sEH inhibitors within the described series.

### Keywords

halogenated pyrazoles; soluble epoxide hydrolase; inhibitor; adamantane; urea

## 1. Introduction

Pyrazole is one of the most used rings in bioactive compounds, including drugs and agrochemicals [1, 2]. It is known that the incorporation of fluoroalkyl groups into organic molecules helps to change their physicochemical properties: changing, among others, pK<sub>a</sub> values of functional groups, increasing metabolic stability, affecting lipophilicity, and enhancing potency and/or selectivity [3–5]. Therefore, fluorinated pyrazole fragments have recently been increasingly used to produce biologically active compounds, such as, for example, well-known anti-inflammatory drug Celecoxib [6], new HIV drug Lenacapavir [7], veterinary drug Deracoxib [8], and fungicide Penflufen [9]. It should be noted that

\*Corresponding author VVB [crus\\_himself@mail.ru](mailto:crus_himself@mail.ru); TKS: [tanya\\_shkineva@mail.ru](mailto:tanya_shkineva@mail.ru).

pyrazoles containing halogen atoms also exhibit a wide range of biological activity [10, 11]. Consequently, the development of methods for the synthesis of new halogenated pyrazoles using a variety of functional groups or structural fragments in order to improve their physicochemical or pharmacological properties is timely and relevant to modern medicinal chemistry.

Soluble epoxide hydrolase (sEH) is an enzyme involved in the metabolism of epoxyeicosatrienoic acids to the corresponding diols [12]. Epoxyeicosatrienoic acids (EETs) are short-lived tissue hormones that regulate many important bodily functions. They have vasodilating and de-aggregation effects, improving microcirculation and promoting tissue repair after myocardial infarction and ischemic stroke. EETs reduce systemic arterial pressure and increase diuresis due to the inhibition of tubular reabsorption of sodium and water in the kidneys. After interacting with PPAR $\alpha$  and PPAR $\gamma$  receptors, these substances realize a clear anti-inflammatory effect [13–16]. Some of the best inhibitors of sEH are compounds containing a ureide fragment in their structure, which mimics the epoxide transition state at the active site of the enzyme (Figure 1). One of the most used moieties in the construction of sEH inhibitors is adamantyl [17, 18]. Although this fragment yields good potency for the sEH inhibition, it also usually results in poor physicochemical properties for the resulting inhibitors, thus limiting their *in vivo* application. Herein, we are testing whether the creation of new inhibitors of sEH, containing both an adamantane and a halogenated pyrazole fragment in their structure, will make it possible to obtain active inhibitors with favorable physicochemical properties.

## 2. Results and discussion

Adamantylisocyanate (**1**, Scheme 1) and adamantylmethylisocyanate (**1'**, Scheme 1) have been used in the reaction with various halogenated aminopyrazoles.

Structures of the obtained chemicals were assessed by NMR, while purity was confirmed by GC-MS, LC-MS, and elemental analysis (see Supplemental materials for details). The structures of compounds **3** and **4** were fully characterized by  $^1\text{H}$  NMR,  $^{13}\text{C}$  NMR,  $^{19}\text{F}$  NMR, IR spectroscopy, HRMS, and elemental analyses. The assignment of pyrazole ring signals was based on well-known trends in the pyrazole series [19–22]. According to these rules the chemical shifts of  $^1\text{H}$  NMR signal for *N*-unsubstituted pyrazoles or their derivatives containing electron-withdrawing *N*-substituents are usually arranged in the following sequence:  $\delta(\text{H-5}) > \delta(\text{H-3}) > \delta(\text{H-4})$ , while the  $^{13}\text{C}$  NMR signal of the C-5 atom is always up-field from the signal of the C-3 atom. In the spectra of compounds **3a-f**  $^1\text{H}$  NMR signals of ureide group lay within the range of 5.62–5.68 ppm (Ad-NH) and 5.91–6.06 ppm (Ad-CH $_2$ -Pyr). The number of fluorine atoms in compounds **3a-c** has almost no effect on NH chemical shifts (5.62–5.64 ppm and 5.91–5.95 ppm). The chemical shifts of  $^{13}\text{C}$  NMR signal for C=O in ureide group of compounds **3a-f** were in the range of 156.5–156.9 ppm. Introduction of methylene group between adamantane fragment and the urea group in compounds **4a-f** moves NH signals downfield to 5.84–5.93 ppm (Ad-NH) and 6.07–6.22 ppm (Ad-CH $_2$ -Pyr) as well as  $^{13}\text{C}$  NMR signal for C=O to 157.9–158.3 ppm due to the decline in electron-donating influence of adamantane fragment.

We also succeeded in obtaining single crystals of 1-[(adamantan-1-yl)methyl]-3-[(1-methyl-5-trifluoromethyl-1H-pyrazol-3-yl)methyl]urea **4e** suitable for the X-ray diffraction study. The single crystals were obtained by slow crystallization from a DMSO solution. Compound **4e** crystallizes in the orthorhombic space group  $Pna2_1$  with one molecule in the asymmetric cell. Notably, the substituted pyrazole fragment appeared to be conformationally disordered into two components with an occupancy of 0.839(3) for the major component. The molecular structure of the main component is shown in Figure 2. The crystal-forming motif in the crystal is a one-dimensional chain formed due to intermolecular hydrogen bonds  $N1-H1 \cdots O1'$  { $N1-H1$  0.86(2) Å,  $H1 \cdots O1'$  2.19(2) Å,  $N1 \cdots O1'$  2.971(2) Å,  $N1-H1 \cdots O1'$  151(2)°; symmetry code  $x+0.5, 0.5-y, z$ } and  $N2-H2 \cdots O1'$  { $N2-H2$  0.865(19) Å,  $H2 \cdots O1'$  2.07(2) Å,  $N2 \cdots O1'$  2.869(2) Å,  $N2-H2 \cdots O1'$  154(2)°; symmetry code  $x+0.5, 0.5-y, z$ } involving only the amide functional groups; this chain is realized along the shortest axis  $0a$  of the unit cell. This supramolecular motif is characteristic of individual ureas that do not contain hydrogen bond donors in side substituents [23].

The physicochemical properties of the synthesized compounds (Table 1) show that the introduction of hydrocarbon spacers between the adamantane fragment and the urea group leads to a decrease in melting points. It should also be noted that an increase in the number of fluorine atoms leads to an increase in the melting point. However, in compounds **4b** and **4c**, the melting point decreases, which is quite likely, due to the greater mobility of the molecule due to the presence of a spacer between the rigid structure of adamantane and the ureide fragment. Compared to previously published adamantyl-urea inhibitors of sEH, the halogenated pyrazoles yield compounds with lower melting point and higher solubility, which will facilitate their formulation. We do not know yet if the compounds will perform better *in vivo*, but in a general manner, introduction of halogens is likely to increase half-life *in vivo* [24].

The calculated lipophilicity coefficient (LogP) for most of the synthesized compounds appears within the Lipinsky rule's limits [25]. The presence of a methylene bridge between the adamantyl radical and the ureide group practically does not change the calculated LogP. The solubility of ureas **3a-f** and **4a-f** are characterized by values in a wide range, from 120 to 750  $\mu\text{M}$ . Compound **4f** has the lowest water solubility (120–130  $\mu\text{M}$ ). The presence of a methylene bridge between the adamantyl radical and the ureide group has no clear effect on water solubility of the synthesized compounds.

The potency of the compounds was then measured against the human sEH. Surprisingly, the presence of a methylene bridge between the ureide group and the adamantyl fragment reduced the activity of the synthesized ureas, although, in earlier works, the presence of a spacer was one of the key factors in increasing activity [26]. It is also worth noting the high activity of compounds in which chlorine atoms are in the pyrazole ring (**3f**,  $\text{IC}_{50} = 0.8$  nM and **4f**,  $\text{IC}_{50} = 1.2$  nM). This is likely due to the electronegativity of chlorine atoms and their effect on the pyrazole ring. Apparently, due to the redistribution of the electron density in the conjugated system, the total charge in pyrazole as a whole also changes.

In compounds **3a** and **3b**, an increase in the number of fluorine atoms reduces the activity (10.2 nM for **3a** and 12.0 nM for **3b**), but already in compound **3c**, which contains a

trifluoromethyl substituent, the activity is higher than that of compound **3a** (9.6 nM for **3c**). The same trend is observed for compounds **4a-c** (13.8 nM for **4a** and 27.5 nM for **4b**), however, the activity of compound **4c** (7.3 nM for **4c**) is almost two times higher than that of compound **4a**.

### 3. Conclusions

A series of soluble epoxide hydrolase (sEH) inhibitors containing various halogenated pyrazole fragments was developed. The inhibition potency of the described compounds ranges from 0.8 to 27.5 nM. The solubility of synthesized ureas lies in a range from 120 to 750  $\mu\text{M}$ . 1-Adamantyl-3-[(4,5-dichloro-1-methyl-1H-pyrazol-3-yl)methyl]urea (**3f**,  $\text{IC}_{50}$  = 0.8 nM) and 1-[(Adamantan-1-yl)methyl]-3-[(4,5-dichloro-1-methyl-1H-pyrazol-3-yl)methyl]urea (**4f**,  $\text{IC}_{50}$  = 1.2 nM) were found to be the most potent sEH inhibitors within the described series.

## 4. Experimental

### 4.1 General methods

Unless otherwise indicated, all common reagents and solvents were used as obtained from commercial suppliers and without further purification. Starting amines **1a-f** were supplied by the Crea-Chim company (<http://www.crea-chim.com>).  $^1\text{H}$ ,  $^{13}\text{C}$ , and  $^{19}\text{F}$  NMR spectra were acquired in Bruker AM 300, Bruker DRX 500, and Bruker AV 600 in  $\text{DMSO}-d_6$  at 298 K. The chemical shift values ( $\delta$ , ppm) of  $^1\text{H}$  and  $^{13}\text{C}$  nuclei were reported relative to TMS, for  $^{19}\text{F}$  nuclei they are relative to  $\text{CFCl}_3$ . The following abbreviations were used to explain multiplicities: s, singlet; br.s, broadened singlet; d, doublet; t, triplet; dt, doublet of triplets; tt, triplet of triplets. Infrared spectra were recorded on a Bruker ALPHA instrument in KBr pellets. The absorptions are given in wavenumbers ( $\text{cm}^{-1}$ ). Melting points were determined by the Kofler method on a Boetius bench (heating rate  $4^\circ\text{C min}^{-1}$ ) and were not corrected. High-resolution mass spectra (HRMS) with electrospray ionization were recorded on a Bruker MicroOTOF II instrument. Elemental analyses were performed by using a CHNS/O Analyzer 2400 (Perkin–Elmer instruments Series II). Analytical TLC was performed using commercially pre-coated silica gel plates (Merck Silicagel 60  $\text{F}_{254}$ ), and visualization was effected with short-wavelength UV light.

X-ray diffraction study of **4e** was performed on a Bruker D8 QUEST diffractometer. Data collected were processed using the *APEX4* software. The structure was solved by the direct method using the *SHELXT* program [29] and refined by the full-matrix least-squares method on  $F^2$  using the *SHELXL* program [30]. Non-hydrogen atoms were refined in the anisotropic approximation. The positions of hydrogen atoms H1 and H2 were determined using difference Fourier maps, and these atoms were refined isotropically. The other hydrogen atoms were inserted in geometrically calculated positions and included in the refinement as riding atoms. Deposition number CCDC 2218618 contains the supplementary crystallographic data for this paper. These data are provided free of charge by the joint Cambridge Crystallographic Data Centre and Fachinformationszentrum Karlsruhe Access Structures service [www.ccdc.cam.ac.uk/structures](http://www.ccdc.cam.ac.uk/structures).

**Crystallographic data for 4e.**— $C_{18}H_{25}F_3N_4O$ , colorless prism ( $0.522 \times 0.206 \times 0.150$  mm<sup>3</sup>), formula weight 370.42 g mol<sup>-1</sup>; orthorhombic, *Pna*2<sub>1</sub> (No. 33),  $a = 9.1405(7)$  Å,  $b = 15.3669(12)$  Å,  $c = 12.5566(10)$  Å,  $V = 1763.7(2)$  Å<sup>3</sup>,  $Z = 4$ ,  $Z' = 1$ ,  $T = 162(2)$  K,  $d_{\text{calc}} = 1.395$  g cm<sup>-3</sup>,  $\mu(\text{Mo } K\alpha) = 0.111$  mm<sup>-1</sup>,  $R(000) = 784$ ;  $T_{\text{max/min}} = 0.9568/0.8239$ ; 33346 reflections were collected ( $2.094^\circ \leq \theta \leq 27.491^\circ$ , index ranges:  $-11 \leq h \leq 11$ ,  $-19 \leq k \leq 19$ , and  $-16 \leq l \leq 16$ ), 4036 of which were unique,  $R_{\text{int}} = 0.0400$ ,  $R_\sigma = 0.0228$ ; completeness to  $\theta$  of  $27.491^\circ$  100.0 %. The refinement of 336 parameters with 515 restraints converged to  $R1 = 0.0335$  and  $wR2 = 0.0795$  for 3640 reflections with  $I > 2\sigma(I)$  and  $R1 = 0.0396$  and  $wR2 = 0.0842$  for all data with goodness-of-fit  $S = 1.062$  and residual electron density  $\rho_{\text{max/min}} = 0.167$  and  $-0.136$  e Å<sup>-3</sup>, rms 0.035; max shift/e.s.d. in the last cycle 0.000.

#### 4.2 General procedure for the synthesis of ureas 3a-f and 4a-f.

To 1 equiv. of corresponding amine **2a-f** in 40 equiv. of DMF was added 1 equiv. of adamantylisocyanate **1** or adamantylmethylisocyanate **1'** and 1 equiv. of Et<sub>3</sub>N (2 equiv. if amine was used in form of hydrochloride) at 0 °C. The reaction mixture was stirred at room temperature for 8 h. After adding 1N HCl and water, the resulting white precipitates were collected by suction filtration.

##### 4.2.1. 1-Adamantyl-3-[[1-(2-fluoroethyl)-1H-pyrazol-3-yl]methyl]urea (3a)—

White solid, Yield 82 mg (23%), mp 155–156 °C. IR (KBr, cm<sup>-1</sup>): 3345 (m), 2908 (m), 2850 (w), 1628 (vs), 1562 (s), 1522 (w), 1360 (w), 1295 (w), 1280 (w), 1238 (w), 1054 (w), 1034 (w), 852 (w), 758 (w), 620 (w) cm<sup>-1</sup>. <sup>1</sup>H NMR (300 MHz, DMSO-*d*<sub>6</sub>)  $\delta$ : 7.64 (1H, c, H-5 Pz); 6.09 (1H, c, H-4 Pz); 5.91 (1H, t,  $J = 5.4$  Hz, NHCH<sub>2</sub>); 5.64 (1H, s, NH); 4.73 (2H, dt, <sup>2</sup> $J_{\text{HF}} = 47.3$  Hz, <sup>3</sup> $J_{\text{HH}} = 4.7$  Hz, CH<sub>2</sub>CH<sub>2</sub>F); 4.35 (2H, dt, <sup>3</sup> $J_{\text{HF}} = 27.7$  Hz, <sup>3</sup> $J_{\text{HH}} = 4.7$  Hz, CH<sub>2</sub>CH<sub>2</sub>F); 4.07 (2H, d,  $J = 5.5$  Hz, NHCH<sub>2</sub>); 1.99 (3H, br.s, CH Ad); 1.86 (6H, br.s, CH<sub>2</sub> Ad); 1.60 (6H, br.s, CH<sub>2</sub> Ad). <sup>19</sup>F NMR (282 MHz, DMSO-*d*<sub>6</sub>)  $\delta$ : -222.39 (tt, <sup>2</sup> $J_{\text{HF}} = 47.3$  Hz, <sup>3</sup> $J_{\text{HF}} = 27.6$  Hz, CH<sub>2</sub>CH<sub>2</sub>F). <sup>13</sup>C NMR (75 MHz, DMSO-*d*<sub>6</sub>)  $\delta$ : 156.9 (C=O); 151.0 (C-3 Pz); 131.3 ((C-5)H Pz); 103.7 ((C-4)H Pz); 80.6 (d, <sup>1</sup> $J_{\text{CF}} = 167.8$  Hz, CH<sub>2</sub>F); 51.5 (d, <sup>2</sup> $J_{\text{CF}} = 19.9$  Hz, CH<sub>2</sub>CH<sub>2</sub>F); 49.5 (CH<sub>2</sub>); 42.0 (CH<sub>2</sub> Ad); 36.9 (C Ad); 36.1 (CH<sub>2</sub> Ad); 28.9 (CH Ad). HRMS (ESI)  $m/z$ : calcd. for C<sub>17</sub>H<sub>26</sub>FN<sub>4</sub>O [M+H]<sup>+</sup>: 321.2085; found 321.2087.

##### 4.2.2 1-Adamantyl-3-[[1-(2,2-difluoroethyl)-1H-pyrazol-3-yl]methyl]urea (3b)—

White solid, Yield 159 mg (42%), mp 148–149 °C. IR (KBr, cm<sup>-1</sup>): 3341 (m), 2905 (s), 2850 (m), 1628 (vs, CO), 1563 (s), 1527 (w), 1360 (w), 1295 (w), 1280 (w), 1240 (w), 1199 (w), 1128 (w), 1074 (m), 1046 (w), 907 (w), 780 (w), 768 (w), 621 (w). <sup>1</sup>H NMR (300 MHz, DMSO-*d*<sub>6</sub>)  $\delta$ : 7.67 (1H, d,  $J = 1.8$  Hz, H-5 Pz); 6.27 (1H, tt, <sup>2</sup> $J_{\text{HF}} = 55.0$  Hz, <sup>3</sup> $J_{\text{HH}} = 3.8$  Hz, CH<sub>2</sub>CHF<sub>2</sub>); 6.14 (1H, d,  $J = 1.8$  Hz, H-4 Pz); 5.93 (1H, t,  $J = 5.6$  Hz, NHCH<sub>2</sub>); 5.62 (1H, s, NH); 4.24 (2H, dt, <sup>3</sup> $J_{\text{HF}} = 15.1$  Hz, <sup>3</sup> $J_{\text{HH}} = 3.8$  Hz, CH<sub>2</sub>CHF<sub>2</sub>); 4.08 (2H, d,  $J = 5.5$  Hz, NHCH<sub>2</sub>); 1.99 (3H, br.s, CH Ad); 1.86 (6H, br.s, CH<sub>2</sub> Ad); 1.60 (6H, br.s, CH<sub>2</sub> Ad). <sup>19</sup>F NMR (282 MHz, DMSO-*d*<sub>6</sub>)  $\delta$ : -123.38 (dt, <sup>2</sup> $J_{\text{HF}} = 55.1$  Hz, <sup>3</sup> $J_{\text{HF}} = 15.0$  Hz, CH<sub>2</sub>CHF<sub>2</sub>). <sup>13</sup>C NMR (75 MHz, DMSO-*d*<sub>6</sub>)  $\delta$ : 156.9 (C=O); 151.7 (C-3 Pz); 132.3 ((C-5)H Pz); 114.1 (t, <sup>1</sup> $J_{\text{CF}} = 241.2$  Hz, CHF<sub>2</sub>); 104.4 ((C-4)H Pz); 52.5 (t, <sup>2</sup> $J_{\text{CF}} = 26.1$  Hz, CH<sub>2</sub>CHF<sub>2</sub>); 49.5 (CH<sub>2</sub>); 42.0 (CH<sub>2</sub> Ad); 36.8 (C Ad); 36.1 (CH<sub>2</sub> Ad); 28.9 (CH Ad). HRMS (ESI)  $m/z$ : calcd. for C<sub>17</sub>H<sub>25</sub>F<sub>2</sub>N<sub>4</sub>O [M+H]<sup>+</sup>: 339.1991; found 339.1984.

**4.2.3 1-Adamantyl-3-[[1-(2,2,2-trifluoroethyl)-1H-pyrazol-3-yl]methyl]urea (3c)**

—White solid, Yield 241 mg (60%), mp 183–184 °C. IR (KBr,  $\text{cm}^{-1}$ ): 3340 (m), 2912 (s), 2850 (m), 1628 (vs, CO), 1565 (s), 1532 (w), 1394 (w), 1295 (w), 1262 (m), 1248 (s), 1169 (s), 1107 (m), 927 (w), 770 (w), 638 (w).  $^1\text{H}$  NMR (300 MHz,  $\text{DMSO}-d_6$ )  $\delta$ : 7.73 (1H, d,  $J = 2.0$  Hz, H-5 Pz); 6.19 (1H, d,  $J = 2.1$  Hz, H-4 Pz); 5.95 (1H, t,  $J = 5.6$  Hz,  $\text{NHCH}_2$ ); 5.63 (1H, s, NH); 5.04 (2H, q,  $^3J_{\text{HF}} = 9.2$  Hz,  $\text{CH}_2\text{CF}_3$ ); 4.09 (2H, d,  $J = 5.6$  Hz,  $\text{NHCH}_2$ ); 1.99 (3H, br.s, CH Ad); 1.86 (6H, br.s,  $\text{CH}_2$  Ad); 1.60 (6H, br.s,  $\text{CH}_2$  Ad).  $^{19}\text{F}$  NMR (282 MHz,  $\text{DMSO}-d_6$ )  $\delta$ : -71.05 (t,  $^3J_{\text{HF}} = 8.8$  Hz,  $\text{CH}_2\text{CF}_3$ ).  $^{13}\text{C}$  NMR (75 MHz,  $\text{DMSO}-d_6$ )  $\delta$ : 156.9 (C=O); 152.4 (C-3 Pz); 132.8 ((C-5)H Pz); 123.6 (q,  $^1J_{\text{CF}} = 279.9$  Hz,  $\text{CF}_3$ ); 105.4 ((C-4)H Pz); 51.2 (q,  $^2J_{\text{CF}} = 33.5$  Hz,  $\text{CH}_2\text{CF}_3$ ); 42.0 ( $\text{CH}_2$  Ad); 38.7 (C Ad); 36.7 ( $\text{CH}_2$  Ad); 28.9 (CH Ad). HRMS (ESI)  $m/z$ : calcd. for  $\text{C}_{17}\text{H}_{24}\text{F}_3\text{N}_4\text{O}$   $[\text{M}+\text{H}]^+$ : 357.1897; found 357.1899.

**4.2.4 1-Adamantyl-3-[(1-difluoromethyl-1H-pyrazol-3-yl)methyl]urea (3d)**

White solid, Yield 224 mg (61%), mp 122–123 °C. IR (KBr,  $\text{cm}^{-1}$ ): 3359 (m), 3307 (m), 2909 (s), 2851 (m), 1631 (vs, CO), 1567 (vs), 1543 (m), 1454 (w), 1381 (m), 1359 (m), 1294 (m), 1279 (m), 1241 (m), 1210 (m), 1114 (m), 1092 (w), 1060 (m), 1048 (s), 989 (w), 823 (s), 758 (w), 624 (w).  $^1\text{H}$  NMR (300 MHz,  $\text{DMSO}-d_6$ )  $\delta$ : 8.10 (1H, d,  $J = 2.3$  Hz, H-5 Pz); 7.14 (1H, t,  $^2J_{\text{HF}} = 59.2$  Hz,  $\text{CHF}_2$ ); 6.34 (1H, d,  $J = 2.3$  Hz, H-4 Pz); 6.06 (1H, t,  $J = 5.6$  Hz,  $\text{NHCH}_2$ ); 5.67 (1H, s, NH); 4.14 (2H, d,  $J = 5.7$  Hz,  $\text{NHCH}_2$ ); 1.99 (3H, br.s, CH Ad); 1.86 (6H, br.s,  $\text{CH}_2$  Ad); 1.60 (6H, br.s,  $\text{CH}_2$  Ad).  $^{19}\text{F}$  NMR (282 MHz,  $\text{DMSO}-d_6$ )  $\delta$ : -94.38 (d,  $^2J_{\text{HF}} = 59.2$  Hz,  $\text{CHF}_2$ ).  $^{13}\text{C}$  NMR (75 MHz,  $\text{DMSO}-d_6$ )  $\delta$ : 156.8 (C=O); 154.8 (C-3 Pz); 130.0 ((C-5)H Pz); 110.1 (t,  $^1J_{\text{CF}} = 247.0$  Hz,  $\text{CHF}_2$ ); 106.8 ((C-4)H Pz); 49.6 ( $\text{CH}_2$ ); 42.0 ( $\text{CH}_2$  Ad); 36.7 (C Ad); 36.1 ( $\text{CH}_2$  Ad); 29.0 (CH Ad). Anal. calcd for  $\text{C}_{16}\text{H}_{22}\text{F}_2\text{N}_4\text{O}$  (324.37): C, 59.24; H, 6.84; N, 17.27; found: C, 59.39; H, 6.96; N 17.29.

**4.2.5 1-Adamantyl-3-[(1-methyl-5-trifluoromethyl-1H-pyrazol-3-yl)methyl]urea (3e)**

White solid, Yield 270 mg (67%), mp 165–166 °C. IR (KBr,  $\text{cm}^{-1}$ ): 3355 (m), 2914 (s), 2853 (m), 1625 (vs, CO), 1565 (s), 1457 (w), 1357 (w), 1293 (w), 1274 (s), 1255 (m), 1185 (s), 1127 (s), 1090 (w), 1039 (w), 620 (w).  $^1\text{H}$  NMR (300 MHz,  $\text{DMSO}-d_6$ )  $\delta$ : 6.64 (1H, s, H-4 Pz); 6.03 (1H, t,  $J = 5.7$  Hz,  $\text{NHCH}_2$ ); 5.64 (1H, s, NH); 4.09 (2H, d,  $J = 5.7$  Hz,  $\text{NHCH}_2$ ); 3.90 (3H, s,  $\text{CH}_3$ ); 1.98 (3H, br.s, CH Ad); 1.86 (6H, br.s,  $\text{CH}_2$  Ad); 1.60 (6H, br.s,  $\text{CH}_2$  Ad).  $^{19}\text{F}$  NMR (282 MHz,  $\text{DMSO}-d_6$ )  $\delta$ : -59.93 (s,  $\text{CF}_3$ ).  $^{13}\text{C}$  NMR (126 MHz,  $\text{DMSO}-d_6$ )  $\delta$ : 156.9 (C=O); 150.6 (C-3 Pz); 130.9 (q,  $^2J_{\text{CF}} = 38.5$  Hz,  $\text{CCF}_3$ ); 120.0 (q,  $^1J_{\text{CF}} = 268.5$  Hz,  $\text{CF}_3$ ); 106.1 ((C-4)H Pz); 49.6 (N $\text{CH}_3$ ); 42.0 ( $\text{CH}_2$  Ad); 37.7 (C Ad); 36.3 ( $\text{CH}_2$ ); 36.2 ( $\text{CH}_2$  Ad); 29.1 (CH Ad). Anal. calcd for  $\text{C}_{17}\text{H}_{23}\text{F}_3\text{N}_4\text{O}$  (356.39): C, 57.29; H, 6.50; N, 15.72; found: C, 57.37; H, 6.58; N, 15.81.

**4.2.6 1-Adamantyl-3-[(4,5-dichloro-1-methyl-1H-pyrazol-3-yl)methyl]urea (3f)**

—White solid, Yield 259 mg (64%), mp 170–171 °C. IR (KBr,  $\text{cm}^{-1}$ ): 3367 (m), 3287 (m), 2905 (s), 2849 (m), 1625 (vs, CO), 1565 (vs), 1520 (m), 1453 (w), 1359 (w), 1293 (m), 1278 (m), 1239 (m), 1132 (w), 1081 (w), 640 (w).  $^1\text{H}$  NMR (300 MHz,  $\text{DMSO}-d_6$ )  $\delta$ : 5.97 (1H, t,  $J = 5.2$  Hz,  $\text{NHCH}_2$ ); 5.68 (1H, s, NH); 4.10 (2H, d,  $J = 4.9$  Hz,  $\text{NHCH}_2$ ); 3.78 (3H, s,  $\text{CH}_3$ ); 1.98 (3H, br.s, CH Ad); 1.85 (6H, br.s,  $\text{CH}_2$  Ad); 1.59 (6H, br.s,  $\text{CH}_2$  Ad).  $^{13}\text{C}$  NMR (75 MHz,  $\text{DMSO}-d_6$ )  $\delta$ : 156.5 (C=O); 146.3 (C-3 Pz); 129.4 (C-5 Pz); 124.6 (C-4 Pz); 49.5 (N $\text{CH}_3$ ); 42.0 ( $\text{CH}_2$  Ad); 37.1 (C Ad); 36.1 ( $\text{CH}_2$  Ad); 35.0 ( $\text{CH}_2$ ); 29.0 (CH Ad). Anal.



calcd for C<sub>16</sub>H<sub>22</sub>Cl<sub>2</sub>N<sub>4</sub>O (357.28): C, 53.79; H, 6.21; N, 15.68; found: C, 53.91; H, 6.40; N, 15.76.

**4.2.7 1-[(Adamantan-1-yl)methyl]-3-[[1-(2-fluoroethyl)-1H-pyrazol-3-yl]methyl]urea (4a)**—White solid, Yield 72 mg (21%),

mp 126–127 °C. IR (KBr, cm<sup>-1</sup>): 3362 (s), 3299 (m), 2907 (s), 2848 (m), 1614 (vs, CO), 1575 (s), 1518 (w), 1468 (w), 1445 (w), 1255 (w), 1062 (w), 1037 (m), 1008 (w), 850 (w), 769 (w), 643 (w), 559 (w), 510 (w). <sup>1</sup>H NMR (300 MHz, DMSO-*d*<sub>6</sub>) δ: 7.66 (1H, d, *J* = 1.8 Hz, H-5 Pz); 6.12 (1H, d, *J* = 1.8 Hz, H-4 Pz); 6.07 (1H, t, *J* = 5.5 Hz, NHCH<sub>2</sub>Pz); 5.87 (1H, t, *J* = 6.0 Hz, NHCH<sub>2</sub>Ad); 4.75 (2H, dt, <sup>2</sup>*J*<sub>HF</sub> = 47.6 Hz, <sup>3</sup>*J*<sub>HH</sub> = 4.8 Hz, CH<sub>2</sub>CH<sub>2</sub>F); 4.37 (2H, dt, <sup>3</sup>*J*<sub>HF</sub> = 27.6 Hz, <sup>3</sup>*J*<sub>HH</sub> = 4.8 Hz, CH<sub>2</sub>CH<sub>2</sub>F); 4.15 (2H, d, *J* = 4.6 Hz, NHCH<sub>2</sub>Pz); 2.74 (2H, d, *J* = 5.4 Hz, NHCH<sub>2</sub>Ad); 1.94 (3H, br.s, CH Ad); 1.63 (6H, dd, *J* = 28.6 Hz, *J* = 12.0 Hz, CH<sub>2</sub> Ad); 1.42 (6H, br.s, CH<sub>2</sub> Ad). <sup>19</sup>F NMR (282 MHz, DMSO-*d*<sub>6</sub>) δ: -222.36 (tt, <sup>2</sup>*J*<sub>HF</sub> = 47.2 Hz, <sup>3</sup>*J*<sub>HF</sub> = 27.5 Hz, CH<sub>2</sub>CH<sub>2</sub>F). <sup>13</sup>C NMR (126 MHz, DMSO-*d*<sub>6</sub>) δ: 158.3 (C=O); 151.0 (C-3 Pz); 131.4 ((C-5)H Pz); 103.7 ((C-4)H Pz); 82.1 (d, <sup>1</sup>*J*<sub>CF</sub> = 167.8 Hz, CH<sub>2</sub>F); 51.5 (d, <sup>2</sup>*J*<sub>CF</sub> = 20.0 Hz, CH<sub>2</sub>CH<sub>2</sub>F); 51.1 (CH<sub>2</sub>); 39.8 (CH<sub>2</sub> Ad); 37.4 (CH<sub>2</sub>); 36.7 (CH<sub>2</sub> Ad); 33.5 (C Ad); 27.8 (CH Ad). Anal. calcd for C<sub>18</sub>H<sub>27</sub>FN<sub>4</sub>O (334.43): C, 64.64; H, 8.14; N, 16.75; found: C, 64.60; H, 8.16; N, 16.71.

**4.2.8 1-[(Adamantan-1-yl)methyl]-3-[[1-(2,2-difluoroethyl)-1H-pyrazol-3-yl]methyl]urea (4b)**

White solid, Yield 157 mg (43%), mp 118–119 °C. IR (KBr, cm<sup>-1</sup>): 3389 (m), 3380 (s), 2904 (vs), 2847 (s), 1614 (vs, CO), 1573 (s), 1522 (m), 1365 (w), 1468 (m), 1243 (m), 1210 (m), 1120 (m), 1069 (vs), 1003 (w), 871 (m), 768 (m), 642 (w), 558 (w), 498 (m). <sup>1</sup>H NMR (300 MHz, DMSO-*d*<sub>6</sub>) δ: 7.69 (1H, d, *J* = 1.9 Hz, H-5 Pz); 6.33 (1H, tt, <sup>2</sup>*J*<sub>HF</sub> = 55.1 Hz, <sup>3</sup>*J*<sub>HH</sub> = 3.8 Hz, CH<sub>2</sub>CHF<sub>2</sub>); 6.17 (1H, d, *J* = 2.0 Hz, H-4 Pz); 6.08 (1H, t, *J* = 5.5 Hz, NHCH<sub>2</sub>Pz); 5.84 (1H, t, *J* = 5.6 Hz, NHCH<sub>2</sub>Ad); 4.56 (2H, dt, <sup>3</sup>*J*<sub>HH</sub> = 3.8 Hz, <sup>3</sup>*J*<sub>HF</sub> = 15.1 Hz, CH<sub>2</sub>CHF<sub>2</sub>); 4.16 (2H, d, *J* = 4.5 Hz, NHCH<sub>2</sub>Pz); 2.74 (2H, d, *J* = 5.9 Hz, NHCH<sub>2</sub>Ad); 1.94 (3H, br.s, CH Ad); 1.64 (6H, dd, *J* = 28.7 Hz, *J* = 11.9 Hz, CH<sub>2</sub> Ad); 1.42 (6H, br.s, CH<sub>2</sub> Ad). <sup>19</sup>F NMR (282 MHz, DMSO-*d*<sub>6</sub>) δ: -123.38 (dt, <sup>2</sup>*J*<sub>HF</sub> = 55.1 Hz, <sup>3</sup>*J*<sub>HF</sub> = 14.9 Hz, CH<sub>2</sub>CHF<sub>2</sub>). <sup>13</sup>C NMR (126 MHz, DMSO-*d*<sub>6</sub>) δ: 158.2 (C=O); 151.8 (C-3 Pz); 132.3 ((C-5)H Pz); 114.1 (t, <sup>1</sup>*J*<sub>CF</sub> = 241.5 Hz, CHF<sub>2</sub>); 104.4 ((C-4)H Pz); 52.5 (t, <sup>2</sup>*J*<sub>CF</sub> = 26.2 Hz, CH<sub>2</sub>CHF<sub>2</sub>); 51.1 (CH<sub>2</sub>); 39.8 (CH<sub>2</sub> Ad); 37.3 (CH<sub>2</sub>); 36.7 (CH<sub>2</sub> Ad); 33.5 (C Ad); 27.8 (CH Ad). Anal. calcd for C<sub>18</sub>H<sub>26</sub>F<sub>2</sub>N<sub>4</sub>O (352.42): C, 61.34; H, 7.44; N, 15.90; found: C, 61.35; H, 7.39; N, 15.83.

**4.2.9 1-[(Adamantan-1-yl)methyl]-3-[[1-(2,2,2-trifluoroethyl)-1H-pyrazol-3-yl]methyl]urea (4c)**

White solid, Yield 247 mg (64%), mp 107–108 °C. IR (KBr, cm<sup>-1</sup>): 3356 (s), 3317 (m), 2908 (vs), 2849 (s), 1609 (vs, CO), 1569 (vs), 1525 (m), 1473 (m), 1393 (w), 1325 (w), 1265 (s), 1203 (w), 1158 (s), 1112 (m), 930 (m), 779 (m), 644 (w). <sup>1</sup>H NMR (300 MHz, DMSO-*d*<sub>6</sub>) δ: 7.75 (1H, br.s, H-5 Pz); 6.22 (1H, br.s, H-4 Pz); 6.12 (1H, br.s, NHCH<sub>2</sub>Pz); 5.89 (1H, br.s, NHCH<sub>2</sub>Ad); 5.06 (2H, q, <sup>3</sup>*J*<sub>HF</sub> = 9.2 Hz, CH<sub>2</sub>CF<sub>3</sub>); 4.16 (2H, br.s, NHCH<sub>2</sub>Pz); 2.74 (2H, d, *J* = 4.5 Hz, NHCH<sub>2</sub>Ad); 1.94 (3H, br.s, CH Ad); 1.64 (6H, dd, *J* = 28.5 Hz, *J* = 12.0 Hz, CH<sub>2</sub> Ad); 1.20 (6H, br.s, CH<sub>2</sub> Ad). <sup>19</sup>F NMR (282 MHz, DMSO-*d*<sub>6</sub>) δ: -71.04 (t, <sup>3</sup>*J*<sub>HF</sub> = 8.4 Hz, CH<sub>2</sub>CF<sub>3</sub>). <sup>13</sup>C NMR (159 MHz, DMSO-*d*<sub>6</sub>) δ: 158.2



(C=O); 152.5 (C-3 Pz); 132.9 ((C-5)H Pz); 123.7 (q,  $^1J_{CF} = 279.7$  Hz, CF<sub>3</sub>); 105.0 ((C-4)H Pz); 51.2 (q,  $^2J_{CF} = 33.4$  Hz, CH<sub>2</sub>CF<sub>3</sub>); 51.0 (CH<sub>2</sub>); 39.8 (CH<sub>2</sub> Ad); 37.4 (CH<sub>2</sub>); 36.7 (CH<sub>2</sub> Ad); 33.5 (C Ad); 27.7 (CH Ad). Anal. calcd for C<sub>18</sub>H<sub>25</sub>F<sub>3</sub>N<sub>4</sub>O (370.41): C, 58.37; H, 6.80; N, 15.13; found: C, 58.40; H, 6.76; N, 15.22.

#### 4.2.10 1-[(Adamantan-1-yl)methyl]-3-[(1-difluoromethyl-1H-pyrazol-3-yl)methyl]jurea (4d)

White solid, Yield 230 mg (65%), mp 113–114 °C. IR (KBr, cm<sup>-1</sup>): 3340 (m), 2915 (s), 2851 (m), 1625 (vs, CO), 1576 (s), 1457 (w), 1380 (m), 1274 (m), 1254 (w), 1212 (m), 1104 (m), 1046 (s), 985 (w), 820 (m), 769 (m), 688 (w). <sup>1</sup>H NMR (300 MHz, DMSO-*d*<sub>6</sub>) δ: 8.13 (1H, d, *J* = 2.4 Hz, H-5 Pz); 7.73 (1H, t,  $^2J_{HF} = 59.2$  Hz, CHF<sub>2</sub>); 6.37 (1H, d, *J* = 2.4 Hz, H-4 Pz); 6.22 (1H, t, *J* = 5.6 Hz, NHCH<sub>2</sub>Pz); 5.93 (1H, t, *J* = 5.9 Hz, NHCH<sub>2</sub>Ad); 4.22 (2H, d, *J* = 4.7 Hz, NHCH<sub>2</sub>Pz); 2.74 (2H, d, *J* = 5.0 Hz, NHCH<sub>2</sub>Ad); 1.94 (3H, br.s, CH Ad); 1.63 (6H, dd, *J* = 28.5 Hz, *J* = 11.9 Hz, CH<sub>2</sub> Ad); 1.42 (6H, br.s, CH<sub>2</sub> Ad). <sup>19</sup>F NMR (282 MHz, DMSO-*d*<sub>6</sub>) δ: -94.40 (d,  $^2J_{HF} = 59.2$  Hz, CHF<sub>2</sub>). <sup>13</sup>C NMR (126 MHz, DMSO-*d*<sub>6</sub>) δ: 158.3 (C=O); 154.8 (C-3 Pz); 130.0 ((C-5)H Pz); 110.1 (t,  $^1J_{CF} = 247.1$  Hz, CHF<sub>2</sub>); 106.7 ((C-4)H Pz); 51.2 (CH<sub>2</sub>); 39.8 (CH<sub>2</sub> Ad); 37.2 (CH<sub>2</sub>); 36.7 (CH<sub>2</sub> Ad); 33.5 (C Ad); 27.8 (CH Ad). Anal. calcd for C<sub>17</sub>H<sub>24</sub>F<sub>2</sub>N<sub>4</sub>O (338.40): C, 60.34; H, 7.15; N, 16.56; found: C, 60.37; H, 7.13; N, 16.48.

#### 4.2.11 1-[(Adamantan-1-yl)methyl]-3-[(1-methyl-5-trifluoromethyl-1H-pyrazol-3-yl)methyl]jurea (4e)

White solid, Yield 265 mg (68%), mp 165–166 °C. IR (KBr, cm<sup>-1</sup>): 3360 (m), 3327 (m); 2908 (s), 2848 (m), 1627 (vs, CO), 1576 (vs), 1458 (m), 1269 (s), 1174 (s), 1145 (w), 1115 (s); 1055 (w), 1031 (w), 807 (w); 669 (w). <sup>1</sup>H NMR (300 MHz, DMSO-*d*<sub>6</sub>) δ: 6.67 (1H, s, H-4 Pz); 6.20 (1H, t, *J* = 5.6 Hz, NHCH<sub>2</sub>Pz); 5.92 (1H, t, *J* = 5.9 Hz, NHCH<sub>2</sub>Ad); 4.17 (2H, d, *J* = 4.9 Hz, NHCH<sub>2</sub>Pz); 3.92 (3H, s, CH<sub>3</sub>); 2.74 (2H, d, *J* = 5.4 Hz, NHCH<sub>2</sub>Ad); 1.93 (3H, br.s, CH Ad); 1.63 (6H, dd, *J* = 30.0 Hz, *J* = 11.9 Hz, CH<sub>2</sub> Ad); 1.42 (6H, br.s, CH<sub>2</sub> Ad). <sup>19</sup>F NMR (282 MHz, DMSO-*d*<sub>6</sub>) δ: -59.98 (s, CF<sub>3</sub>). <sup>13</sup>C NMR (151 MHz, DMSO-*d*<sub>6</sub>) δ: 158.3 (C=O); 150.7 (C-3 Pz); 131.0 (q,  $^2J_{CF} = 38.4$  Hz, CCF<sub>3</sub>); 120.1 (q,  $^1J_{CF} = 268.5$  Hz, CF<sub>3</sub>); 106.1 ((C-4)H Pz); 51.3 (NCH<sub>3</sub>); 39.9 (CH<sub>2</sub> Ad); 37.7 (CH<sub>2</sub>); 36.9 (CH<sub>2</sub>); 36.7 (CH<sub>2</sub> Ad); 33.6 (C Ad); 27.9 (CH Ad). Anal. calcd for C<sub>18</sub>H<sub>25</sub>F<sub>3</sub>N<sub>4</sub>O (370.41): C, 58.37; H, 6.80; N, 15.13; found: C, 58.37; H, 6.80; N, 15.13.

#### 4.2.12 1-[(Adamantan-1-yl)methyl]-3-[(4,5-dichloro-1-methyl-1H-pyrazol-3-yl)methyl]jurea (4f)

White solid, Yield 253 mg (64%), mp 127–128 °C. IR (KBr, cm<sup>-1</sup>): 3341 (m), 2901 (s), 2848 (m), 1626 (vs, CO), 1577 (vs), 1523 (m), 1450 (m), 1378 (w), 1243 (m), 1188 (w), 1132 (w), 676 (m), 650 (w); 565 (w). <sup>1</sup>H NMR (300 MHz, DMSO-*d*<sub>6</sub>) δ: 6.12 (1H, br.s, NHCH<sub>2</sub>Pz); 5.92 (1H, br.s, NHCH<sub>2</sub>Ad); 4.18 (2H, d, *J* = 3.8 Hz, NHCH<sub>2</sub>Pz); 3.80 (3H, s, CH<sub>3</sub>); 2.72 (2H, d, *J* = 4.9 Hz, NHCH<sub>2</sub>Ad); 1.93 (3H, br.s, CH Ad); 1.63 (6H, dd, *J* = 39.1 Hz, *J* = 11.9 Hz, CH<sub>2</sub> Ad); 1.41 (6H, br.s, CH<sub>2</sub> Ad). <sup>13</sup>C NMR (151 MHz, DMSO-*d*<sub>6</sub>) δ: 157.9 (C=O); 146.3 (C-3 Pz); 129.5 (C-5 Pz); 104.7 (C-4 Pz); 51.1 (NCH<sub>3</sub>); 39.8 (CH<sub>2</sub> Ad); 37.1 (CH<sub>2</sub>); 36.7 (CH<sub>2</sub> Ad); 35.5 (CH<sub>2</sub>); 33.5 (C Ad); 27.7 (CH Ad). Anal. calcd for C<sub>17</sub>H<sub>24</sub>Cl<sub>2</sub>N<sub>4</sub>O (371.30): C, 54.99; H, 6.52; N, 15.09; found: C, 55.09; H, 6.41; N, 15.01.

### 4.3 Determination of inhibitory potency (IC<sub>50</sub>) by fluorescent assay [27].

The enzyme (ca. 1 nM human sEH) was incubated at 30 °C with inhibitors ( $[I]_{\text{final}} = 0.4\text{--}100,000$  nM) for 5 min in 100 mM sodium phosphate buffer (200  $\mu\text{L}$ , pH 7.4) containing 0.1 mg mL<sup>-1</sup> of BSA and 1% of DMSO. The substrate (cyano(2-methoxynaphthalen-6-yl)methyl *trans*-(3-phenyloxyran-2-yl)methylcarbonate, CMNPC) was then added ( $[S]_{\text{final}} = 5$   $\mu\text{M}$ ). The activity was assessed by measuring the appearance of the fluorescent 6-methoxynaphthaldehyde product ( $\lambda_{\text{em}} = 330$  nm,  $\lambda_{\text{ex}} = 465$  nm) at 30 °C during a 10 min incubation (Spectramax M2; Molecular Device, Inc., Sunnyvale, CA). The IC<sub>50</sub> values, which are the concentrations of inhibitors that reduce activity by 50 %, were calculated from at least five different concentrations, each in triplicate, with at least 2 on either side of 50 % activity mark.

## Supplementary Material

Refer to Web version on PubMed Central for supplementary material.

## Acknowledgments

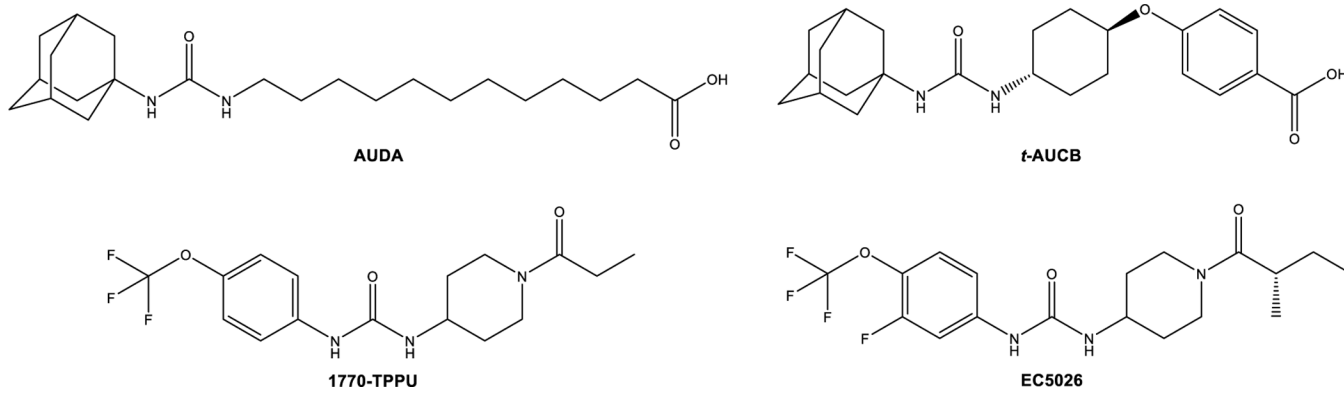
This work was supported by the Russian Science Foundation (grant number 21-73-20123) and, in part, by National Institute of Environmental Health Sciences (NIEHS) grant R35 ES030443. R. R. F. performed crystal structure determination within the government statements for Kazan Scientific Center of RAS. X-ray diffraction data were registered on the equipment of the Distributed Spectral-Analytical Center of Shared Facilities for Study of Structure, Composition and Properties of Substances and Materials of FRC Kazan Scientific Center of RAS.

## References

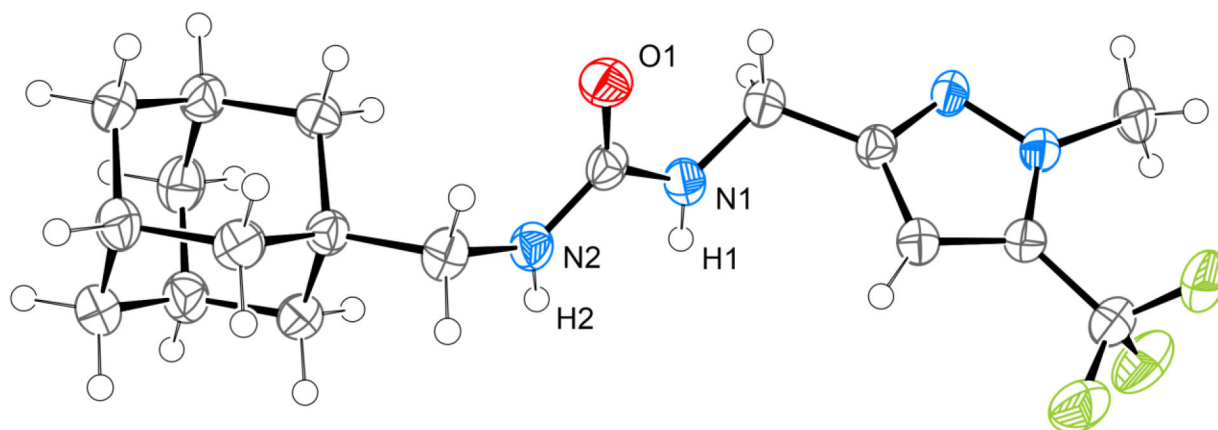
1. Faria JV, Vegi PF, Miguita AGC, dos Santos MS, Boechat N, Bernardino AMR, Recently reported biological activities of pyrazole compounds, *Bioorg. Med. Chem.* 25 (2017) 5891–5903, 10.1016/j.bmc.2017.09.035. [PubMed: 28988624]
2. Taylor RD, MacCoss M, Lawson ADG, Rings in Drugs, *J. Med. Chem.* 57 (2014) 5845–5859, 10.1021/jm4017625. [PubMed: 24471928]
3. Gillis EP, Eastman KJ, Hill MD, Donnelly DJ, Meanwell NA, Applications of Fluorine in Medicinal Chemistry, *J. Med. Chem.* 58 (2015) 8315–8359, 10.1021/acs.jmedchem.5b00258. [PubMed: 26200936]
4. Meanwell NA, Fluorine and Fluorinated Motifs in the Design and Application of Bioisosteres for Drug Design, *J. Med. Chem.* 61 (2018) 5822–5880, 10.1021/acs.jmedchem.7b01788. [PubMed: 29400967]
5. Zhou Y, Wang J, Gu Z, Wang S, Zhu W, Aceña JL, Soloshonok VA, Izawa K, Liu H, Next Generation of Fluorine-Containing Pharmaceuticals, Compounds Currently in Phase II–III Clinical Trials of Major Pharmaceutical Companies: New Structural Trends and Therapeutic Areas, *Chem. Rev.* 116 (2016) 422–518, 10.1021/acs.chemrev.5b00392. [PubMed: 26756377]
6. Penning TD, Talley JJ, Bertenshaw SR, Carter JS, Collins PW, Docter S, Graneto MJ, Lee LF, Malecha JW, Miyashiro JM, Rogers RS, Rogier DJ, Yu SS, Anderson GD, Burton EG, Cogburn JN, Gregory SA, Koboldt CM, Perkins WE, Seibert K, Veenhuizen AW, Zhang YY, Isakson PC, Synthesis and Biological Evaluation of the 1,5-Diarylpyrazole Class of Cyclooxygenase-2 Inhibitors: Identification of 4-[5-(4-Methylphenyl)-3-(trifluoromethyl)-1H-pyrazol-1-yl]benzenesulfonamide (SC-58635, Celecoxib), *J. Med. Chem.* 40 (1997) 1347–1365, 10.1021/jm960803q. [PubMed: 9135032]
7. Link JO, Rhee MS, Tse WC, Zheng J, Somoza JR, Rowe W, Begley R, Chiu A, Mulato A, Hansen D, Singer E, Tsai LK, Bam RA, Chou C-H, Canales E, Brizgys G, Zhang JR, Li J, Graupe M, Morganelli P, Liu Q, Wu Q, Halcomb RL, Saito RD, Schroeder SD, Lazerwith SE, Bondy S, Jin D, Hung M, Novikov N, Liu X, Villaseñor AG, Cannizzaro CE, Hu EY, Anderson RL, Appleby

- TC, Lu B, Mwangi J, Liclican A, Niedziela-Majka A, Papalia GA, Wong MH, Leavitt SA, Xu Y, Koditek D, Stepan GJ, Yu H, Pagratis N, Clancy S, Ahmadyar S, Cai TZ, Sellers S, Wolckenhauer SA, Ling J, Callebaut C, Margot N, Ram RR, Liu Y-P, Hyland R, Sinclair GI, Ruane PJ, Crofoot GE, McDonald CK, Brainard DM, Lad L, Swaminathan S, Sundquist WI, Sakowicz R, Chester AE, Lee WE, Daar ES, Yan SR, Cihlar T, Clinical targeting of HIV capsid protein with a long-acting small molecule, *Nature* 584 (2020) 614–618, 10.1038/s41586-020-2443-1. [PubMed: 32612233]
8. Spyra S, Meisner A, Schaefer M, COX-2-selective inhibitors celecoxib and deracoxib modulate transient receptor potential vanilloid 3 channels, *Brit. J. Pharmacol.* 174 (2017) 2696–2705, 10.1111/bph.13893. [PubMed: 28567799]
  9. Di S, Wang Z, Cang T, Xie Y, Zhao H, Qi P, Wang X, Xu H, Wang X, Enantioselective toxicity and mechanism of chiral fungicide penflufen based on experiments and computational chemistry, *Ecotoxicol. Environ. Saf.* 222 (2021), 112534, 10.1016/j.ecoenv.2021.112534. [PubMed: 34311429]
  10. Schmidt A, Dreger A, Recent Advances in the Chemistry of Pyrazoles. Properties, Biological Activities, and Syntheses, *Current Org. Chem.* 15 (2011) 1423–1463, 10.2174/138527211795378263.
  11. Jeschke P, Latest generation of halogen-containing pesticides, *Pest. Manag. Sci.* 73 (2017) 1053–1066, 10.1002/ps.4540. [PubMed: 28145087]
  12. Arand M, Grant DF, Beetham JK, Friedberg T, Oesch F, Hammock BD, Sequence similarity of mammalian epoxide hydrolases to the bacterial haloalkane dehalogenase and other related proteins. Implication for the potential catalytic mechanism of enzymatic epoxide hydrolysis, *FEBS Lett.* 338 (1994) 251–256, 10.1016/0014-5793(94)80278-5. [PubMed: 8307189]
  13. Spector AA, Fang X, Snyder GD, Weintraub NL, Epoxyeicosatrienoic acids (EETs): metabolism and biochemical function, *Prog. Lipid Res.* 43 (2004) 55–90, 10.1016/S0163-7827(03)00049-3. [PubMed: 14636671]
  14. Oni-Orisan A, Alsaleh N, Lee CR, Seubert JM, Epoxyeicosatrienoic acids and cardioprotection: The road to translation, *J. Mol. Cell. Cardiol.* 74 (2014) 199–208, 10.1016/j.yjmcc.2014.05.016. [PubMed: 24893205]
  15. Tacconelli S, Patrignani P, Inside epoxyeicosatrienoic acids and cardiovascular disease, *Front. Pharmacol.* 5 (2014) 239, 10.3389/fphar.2014.00239. [PubMed: 25426071]
  16. Huang H, Al-Shabrawey M, Wang MH, Cyclooxygenase- and cytochrome P450-derived eicosanoids in stroke, *Prostaglandins Other Lipid Mediat.* 122 (2016) 45–53, 10.1016/j.prostaglandins.2015.12.007. [PubMed: 26747234]
  17. Burmistrov V, Morisseau C, D'yachenko V, Rybakov VB, Butov GM, Hammock BD, Fluoroaromatic fragments on 1,3-disubstituted ureas enhance soluble epoxide hydrolase inhibition, *J. Fluor. Chem.* 220 (2019) 48–53, 10.1016/j.jfluchem.2019.02.005. [PubMed: 32132741]
  18. North EJ, Scherman MS, Bruhn DF, Scarborough JS, Maddox MM, Jones V, Grzegorzewicz A, Yang L, Hess T, Morisseau C, Jackson M, McNeil MR, Lee RE, Design, Synthesis and Anti-tuberculosis Activity of 1-Adamantyl-3-heteroaryl Ureas with Improved in vitro Pharmacokinetic Properties, *Bioorg. Med. Chem.* 21 (2013) 2587–2599, 10.1016/j.bmc.2013.02.028. [PubMed: 23498915]
  19. Zaitsev AA, Dalinger IL, Shevelev SA, Dinitropyrazoles, *Russ. Chem. Rev.* 78 (2009) 589–627, 10.1070/RC2009v078n07ABEH004015.
  20. Khoranyan TE, Shkineva TK, Vatsadze IA, Shakhnes A.Kh., Muravyev NV, Sheremetev AB, Dalinger IL, Regioisomeric 3,5-di(nitropyrazolyl)-1,2,4-oxadiazoles and their energetic properties, *Chem. Heterocycl. Compd.* 58 (2022) 37–44, 10.1007/s10593-022-03054-1.
  21. Kormanov AV, Shkineva TK, Dalinger IL, Acetylation of 5(3)-(1H-tetrazol-1-yl)-3(5)-nitro-1H-pyrazole, *Mendeleev Commun.* 27 (2017) 462–463, 10.1016/j.mencom.2017.09.010.
  22. Dalinger IL, Kormanov AV, Vatsadze IA, Serushkina OV, Shkineva TK, Suponitsky K.Yu., Pivkina AN, Sheremetev AB, Synthesis of 1- and 5-(pyrazolyl)tetrazole amino and nitro derivatives, *Chem. Heterocycl. Compd.* 52 (2016) 1025–1034, 10.1007/s10593-017-2003-2.
  23. Litvinov IA, Burmistrov VV, Fayzullin RR, Structure of Some Adamantyl-Containing Ureas and Hydrogen Bonds in Their Crystals, *J. Struct. Chem.* 63 (2022) 1274–1283, 10.1134/S002247662208008X.

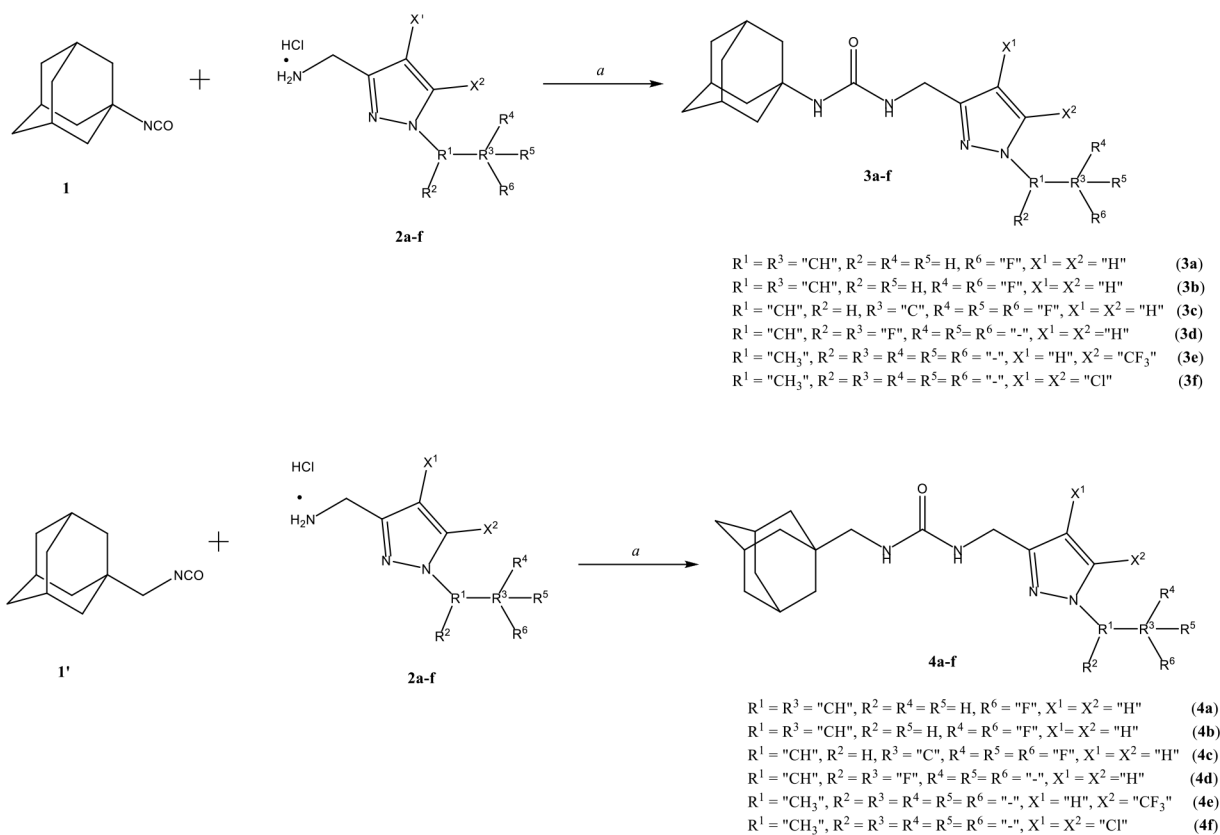
24. Gunaydin H, Altman MD, Ellis JM, Fuller P, Johnson SA, Lahue B, Lapointe B, Strategy for Extending Half-life in Drug Design and Its Significance, *ACS Med. Chem. Lett.* 9 (2018) 528–533, 10.1021/acsmchemlett.8b00018. [PubMed: 29937977]
25. Lipinski CA, Lombardo F, Dominy BW, Feeney PJ, Experimental and computational approaches to estimate solubility and permeability in drug discovery and development settings, *Adv. Drug Del. Rev.* 46 (2001) 3–26, 10.1016/S0169-409X(00)00129-0.
26. Burmistrov V, Morisseau C, Harris TR, Butov GM, Hammock BD, Effects of adamantane alterations on soluble epoxide hydrolase inhibition potency, physical properties and metabolic stability, *Bioorg. Chem.* 76 (2018) 510–527, 10.1016/j.bioorg.2017.12.024. [PubMed: 29310082]
27. Jones PD, Wolf NM, Morisseau C, Whetstone P, Hock B, Hammock BD, Fluorescent substrates for soluble epoxide hydrolase and application to inhibition studies, *Anal. Biochem.* 343 (2005) 66–75, 10.1016/j.ab.2005.03.041. [PubMed: 15963942]
28. Hwang SH, Tsai H-J, Liu J-Y, Morisseau C, Hammock BD, Orally Bioavailable Potent Soluble Epoxide Hydrolase Inhibitors, *J. Med. Chem.* 50 (2007) 3825–3840, 10.1021/jm070270t. [PubMed: 17616115]
29. Sheldrick GM, SHELXT – Integrated Space-Group and Crystal-Structure Determination, *Acta Crystallogr., Sect. A: Found. Crystallogr.* 71 (2015) 3–8, 10.1107/S2053273314026370.
30. Sheldrick GM, Crystal Structure Refinement with SHELXL, *Acta Crystallogr., Sect. C: Struct. Chem.* 71 (2015) 3–8, 10.1107/S2053229614024218. [PubMed: 25567568]



**Figure 1.**  
Known potent soluble epoxide hydrolase inhibitors.



**Figure 2.** ORTEP of urea 4e in the crystal at the 50 % probability level for non-hydrogen atoms. The minor disorder component is omitted for clarity.

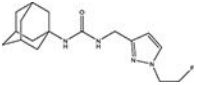
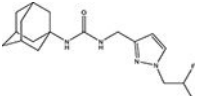
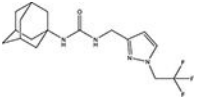
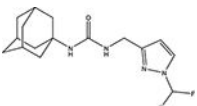
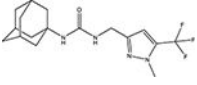
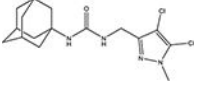
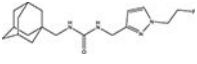
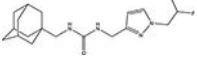
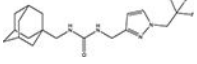
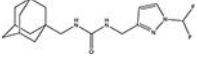
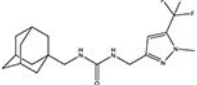
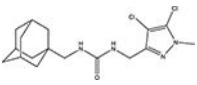
**Scheme 1.**

Synthesis of compounds 3 and 4. Reagents and conditions: a. DMF, Et<sub>3</sub>N (2 equiv.), 8 h., room temperature.



**Table 1**

Properties of compounds 3a-f and 4a-f

#	Structure	LogP calc <sup>a</sup>	mp (°C)	Solubility (μM) <sup>b</sup>
3a		3.06	155–156	440–450
3b		3.33	148–149	300–310
3c		3.69	183–184	390–400
3d		3.32	122–123	670–680
3e		3.89	165–166	160–170
3f		4.17	170–171	250–260
4a		3.07	126–127	650–660
4b		3.34	118–119	270–280
4c		3.70	107–108	740–750
4d		3.33	113–114	570–580
4e		3.91	165–166	160–170
4f		4.18	127–128	120–130

<sup>a</sup>Calculated using Molinspiration (<http://www.molinspiration.com>) © Molinspiration Cheminformatics.

<sup>b</sup>Solubilities were measured in sodium phosphate buffer (pH 7.4, 0.1 M) containing 1% of DMSO.

Author Manuscript

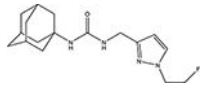
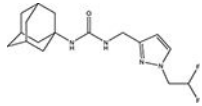
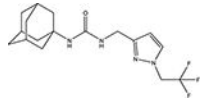
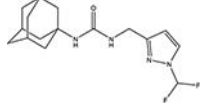
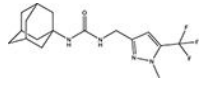
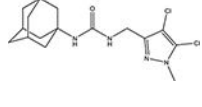
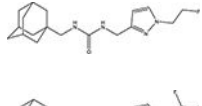
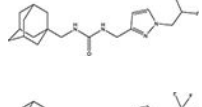
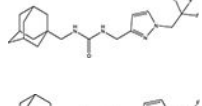
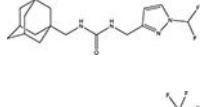
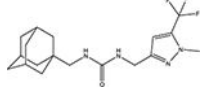
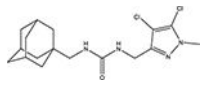
Author Manuscript

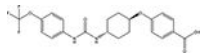
Author Manuscript

Author Manuscript

Table 2

IC<sub>50</sub> values for compounds **3a-f** and **4a-f**.

#	Structure	IC <sub>50</sub> (nM) <sup>d</sup>
<b>3a</b>		10.2
<b>3b</b>		12.0
<b>3c</b>		9.6
<b>3d</b>		8.8
<b>3e</b>		9.9
<b>3f</b>		0.8
<b>4a</b>		13.8
<b>4b</b>		27.5
<b>4c</b>		7.3
<b>4d</b>		15.0
<b>4e</b>		22.5
<b>4f</b>		1.2

#	Structure	IC <sub>50</sub> (nM) <sup>a</sup>
<i>t</i> -TUCB <sup>b</sup>		0.9

<sup>a</sup>Determined via a kinetic fluorescent assay (Concentration of substrate 5 μM, concentration of human sEH 1 nM) [27]. Results are means of three separate experiments.

<sup>b</sup>Used as positive control [28].

Author Manuscript

Author Manuscript

Author Manuscript

Author Manuscript